# Inception Criteria for Droplet Entrainment In Two-Phase Concurrent Film Flow

Inception criteria for droplet entrainment in concurrent gas-liquid film flow were developed from simple physical models. For film Reynolds number $\gtrsim$ 160, an entrainment model based on the shearing off of roll-wave crests was used. At lower film Reynolds numbers, a wave undercutting mechanism was introduced. Experimentally observed abrupt changes in the critical gas velocity corresponding to the onset of entrainment at a certain film Reynolds number have been explained by the shift in the entrainment mechanisms. An agreement of the present inception criteria with various experimental data is shown to be satisfactory, and significant improvements over the existing empirical correlations have been made.

**M. ISHII and**

**M. A. GROLMES**

**Reactor Analysis and Safety Division**
**Argonne National Laboratory**
**9700 South Cass Avenue**
**Argonne, Illinois 60439**

## SCOPE

An understanding of the conditions leading to entrainment and atomization of a liquid film by a gas flow is of considerable practical importance for heat and mass transfer processes in two-phase flow systems. The mechanisms of mass, momentum, and energy transfer between the film and gas core flow is significantly altered by the inception of entrainment.

For example, the "burnout and post-burnout" heat flux in light-water cooled nuclear reactors (Collier, 1961; Petrovichev et al., 1971; Cousins et al., 1965), the effectiveness of the emergency core cooling systems in water reactors (Semeria and Martinet, 1965; Yamanouchi, 1968; Duffey, 1973), and the performance of the film cooling of jet and rocket engines (Kinney et al., 1957; Knuth, 1954) can be significantly affected by the entrainment of the liquid film into the gas core flow. We also note that the prediction of sodium film and cladding relocation in the liquid metal fast breeder reactors (Henry et al., 1974; Grolmes et al., 1974) as well as gas-cooled fast reactors under accident conditions could be affected by a reliable entrainment criterion. Numerous other examples where the atomization and entrainment of the liquid film imposes operational and performance limitations could be found in various chemical engineering systems (Zuber, 1962; Brodkey, 1967; Pushkina and Sorokin, 1969).

The comparison of the various experimental data and the existing correlations (van Rossum, 1959; Kutateladze, 1972; Chien and Ibele, 1960; Zhivaikin, 1962; Steen and Wallis, 1964) showed several discrepancies (see Figure 1 and Figure 3). Since these correlations are purely empirical formulas, a physical understanding of the initiation of entrainment cannot be obtained from them. Furthermore, the generality of some correlations (van Rossum, 1959; Zhivaikin, 1962) is in serious question due to their dimensional forms. On the other hand, the nondimensional correlations (Kutateladze, 1972; Steen and Wallis, 1964) fit only to the part of the characteristics of experimental data, and therefore they can be considered as overly simplified models. In view of these shortcomings of existing empirical correlations, it is highly desirable to obtain an entrainment inception criterion based upon physical modeling which can provide some understanding of the entrainment mechanisms and a reliable design rule. This is particularly important for liquid metal systems such as sodium and molten stainless steel where conventional empirical correlations appear not applicable. The purpose of this paper is to develop such inception criteria from physical models based on two dominant entrainment mechanisms, that is, shearing off of a roll-wave crest and undercutting of a liquid film. Furthermore, an effort has been made to explain seemingly contradicting experimental results from various investigators by a unified inception criteria.

## CONCLUSIONS AND SIGNIFICANCE

It has been shown that for a concurrent two-phase film flow system, there are several possible mechanisms of a droplet entrainment by a high velocity gas flow. New inception criteria for entrainment were obtained from the simple physical models. The mechanism of shearing off of a roll-wave crest was used to obtain the criterion for relatively high film Reynolds number regimes. The critical velocity at the onset of entrainment depends on the viscosity number $N_\mu$ and the film Reynolds number $Re_f$. However, for a completely rough turbulent regime, for example, $Re_f \geq 1635$, the asymptotic criterion is independent of the Reynolds number.

In the lower Reynolds number regime, the entrainment mechanism based on the wave undercutting by a turbulent gas flow was postulated and the criteria for the inception of entrainment was deduced from the analogy with the Hinze's droplet disintegration model. Rather abrupt changes in the critical gas velocity at a certain film Reynolds number have been explained by the shift in the above two different entrainment mechanisms. In addition, the minimum film Reynolds number, below which no entrainment is possible irrespective of the gas velocity, has been proposed and the criterion was derived from the physical model based on the submergence of the film in the gas turbulent boundary layer.

The comparison of the present models to the wide variety of experimental data has been given and the agreement between them are satisfactory. A partial explanation of the seemingly contradicting experimental results of various investigators is possible from the present theory.

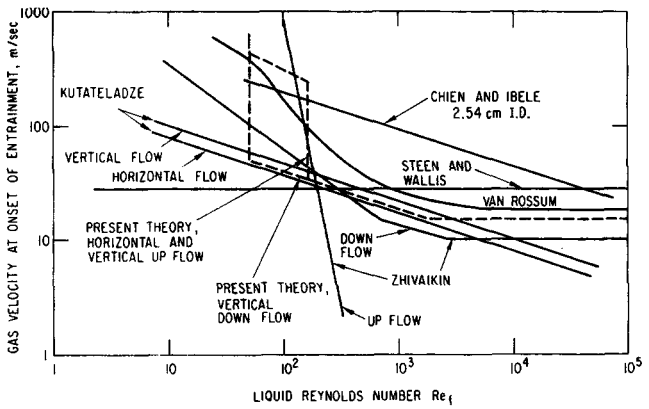


**Fig. 1. Comparison of various entrainment correlations for water-air flow at 15°C.**

In a system where a liquid phase flows along the wall as a film with a gas phase flowing over it, several transitions in hydrodynamic characteristics take place before the onset of the liquid entrainment (Brodkey, 1967; van Rossum, 1959; Levich, 1962; Hewitt and Hall-Taylor, 1970; Wallis, 1969; Lamb, 1945). When the gas velocity is sufficiently small, the interface appears to be relatively stable. Although there have been some conflicting results on the absolute stability of the vertical films in terms of the liquid Reynolds number, it can be said in general that for increased gas velocity the interface becomes wavy due to the well-known Kelvin-Helmholtz instability (Levich, 1962; Lamb, 1945). In horizontal or inclined channels, the gravity and surface tension force has a stabilizing effect, whereas the relative velocity between the phases destabilizes the film by variation in pressure distribution over the wave. At the wave crest the gas velocity is higher corresponding to a lower pressure according to the Bernoulli theorem, and at the wave trough the lower gas velocity results in a higher gas pressure. When the film is unstable the dominant waves to appear are the ones having the maximum growth factor. The order of magnitude of this wave length is characterized by $\sigma/(\rho_g v_r^2)$ which is generally small compared with other types of interfacial waves (Levich, 1962; Lamb, 1945), thus Rayleigh called these capillary waves *ripples*.

As the relative velocity is further increased, the waves become irregular and three-dimensional (van Rossum, 1959; Hanratty and Hershman, 1961). At a sufficiently high wave amplitude and gas velocity, these capillary waves having the characteristic of dynamic waves can transform to large amplitude kinematic waves (Lighthill and Whitham, 1955), which propagate in one direction. These are the roll waves studied by Hanratty and Hershman (1961) among others (Hanratty and Engen, 1957; Chung and Murgatroyd, 1965). At the roll wave transition (Brodkey, 1967; Hanratty and Hershman, 1961) or at a still higher gas velocity (Wallis, 1969) the onset of the entrainment has been observed. However, the experimental work of van Rossum (1959) suggests that the entrainment can also occur in the absence of large amplitude roll waves for a highly viscous fluid.

Reviews of existing experimental and analytical work on the inception of liquid entrainment have been carried out by Zuber (1962), Hewitt and Hall-Taylor (1970), Wallis (1969), and Kutateladze (1972). Zuber's work was also directed to explore possible entrainment mechanisms. By using simple models based on force balances, several similarity criteria are derived in Zuber (1962). The extensive review work of Hewitt and Hall-Taylor (1970) summarizes various experimental data and correlations. It has been shown there that large discrepancies exist among the various correlations and also between the experimental data. For example, the critical gas velocity predicted by the correlation of Chien and Ibele (1960) can be five times as high as the one given by Zhivaikin (1962) (see Figure 1). These results are not surprising since several completely different methods of defining the experimental point of entrainment inception have been used. Experimental results based on sampling probes (Cousins et al., 1965; Steen and Wallis, 1964; Wallis, 1962; Yablonik and Khaimov, 1972; Ueda and Tanaka, 1973) show that the mass fraction entrained increases rather slowly with increasing gas velocity near the inception point. Furthermore, the position of the curve can be easily shifted at the low entrainment region by changing the inlet conditions or by changing the position of the sampling probes. However, at a relatively high entrainment fraction, it increases linearly with the gas velocity. Consequently, some investigators (Steen and Wallis, 1964; Wallis, 1962; Yablonik and Khaimov, 1972) used the linear extrapolation from the high entrainment fraction region to the zero entrainment condition, as shown in Figure 2.

In contrast to the linear extrapolation method, Cousins et al. (1965) and Ueda and Tanaka (1973) carefully followed the actual entrainment curve by measuring the liquid fraction entrained at lower gas velocities; thus it can be expected that their data indicate smaller critical gas velocities than those of Steen and Wallis (1964), Wallis (1962), and Yablonik and Khaimov (1972). The differences between the critical gas velocity at the actual onset, and the one based on the linear extrapolation method can be as high as 100% even under controlled inlet condition, which effectively eliminated the entrainment caused by liquid injection to the system. It was also pointed out in Cousins et al. (1965), Wallis (1969), and Yablonik and Khaimov (1972) that the measured critical gas velocity depends on the axial and transverse position of the sampling probe, which further complicates the procedure to define the experimental point of the onset of entrainment.

Apart from the sampling method, several different entrainment detection methods and inception criteria have been used. Visual observations (van Rossum, 1959; Zhivaikin, 1962) as well as pressure drop measurements (Chien and Ibele, 1960; Zhivaikin, 1962) are useful means to identify the change in the flow regimes or in the interfacial characteristics. In general, two transition points in the pressure drop versus gas flow curve can be observed, that is, one associated with the smooth film to wavy film transi-

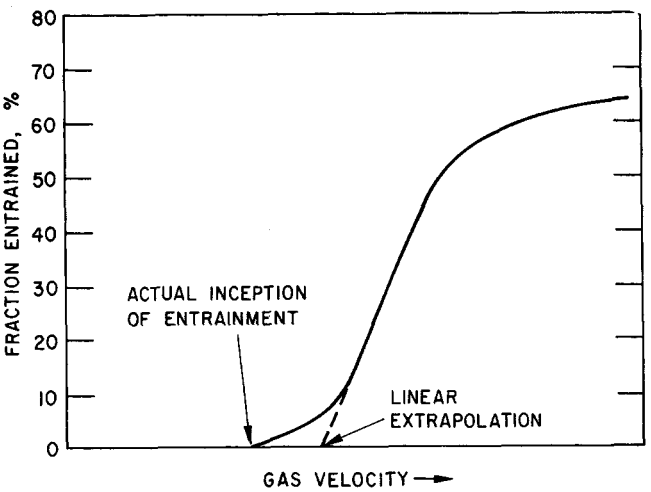


**Fig. 2. Typical relation between fraction of liquid entrained and gas velocity at constant liquid flow rate.**

tion and the other with the onset of entrainment. Both transitions are characterized by an increase in the pressure drop gradient signifying a change in momentum transfer mechanisms. In spite of the several existing methods, the difficulties encountered in deciding the entrainment inception point are noted by various investigators (Hewitt and Hall-Taylor, 1970; Wallis, 1962; Yablonik and Khaimov, 1972). Further discussions concerning the film flow measurements can be found elsewhere (Hewitt and Hall-Taylor, 1970).

There are also conflicting results on the effects of direction of the flows, that is, horizontal, vertical upwards, and vertical downwards flows (see Figure 1). Zhivaikin's experiment (1962) shows that the inception of droplet entrainment depends on the flow direction at least at the low liquid Reynolds number region, whereas Wallis' result (1962) indicates that the onset is independent of the flow orientation. In contrast, the correlations proposed by Kutateladze (1970) depend on the flow direction over the whole range of liquid Reynolds number.

In countercurrent film flow, the situation is further complicated by the flooding phenomenon. Near the flooding point, the interface is extremely unstable and large amplitude waves appear. These waves can be carried up by a gas flow or in small diameter channels extend to form a liquid bridge which can be entrained into the gas stream. The mechanism of entrainment can be quite different in this case from the one occurring in a concurrent gas-liquid flows (refer to Figure 7, type 5).

Detailed experimental work using various liquids was carried out by van Rossum (1959). His data indicate that there exist several different mechanisms of entrainment. He was apparently the first to realize that for sufficiently high liquid film Reynolds numbers, the critical gas velocity approaches a constant value which he correlated in terms of the liquid surface tension parameter. His empirical rule, however, has a dimensional form and its general use is questionable, particularly for liquid metals. At smaller Reynolds numbers, the experimental data appear to converge to a single curve when they are plotted in the dimensionless plane of the liquid Reynolds number versus $v_g\mu_f/\sigma$ or in the plane of Weber number versus $v_g\mu_f/\sigma$, which van Rossum presented as a graphical correlation.

The experimental results of Zhivaikin (1962) for a concurrent downward flow were expressed by three correlations in terms of the liquid Reynolds number. The generality of these correlations is also questionable owing to their dimensional form. Steen and Wallis (1964) examined the effects of inlet conditions on the onset of entrainment as well as the effects of the tube diameter. The liquid properties and the gas density have been changed, however, due to their liquid injection method, the experiment tends to produce high inlet entrainment. Thus, it is quite difficult to detect the precise point of entrainment inception. The correlation proposed by Steen is independent of the liquid Reynolds number, but it includes the density ratio of the gas and the liquid. In view of the experimental observations of Zhivaikin (1962) and van Rossum (1959), it can be concluded that the correlation of Steen and Wallis (1964) is applicable only at relatively large Reynolds number. Furthermore, because of the method to define the inception point, the correlation tends to give a larger gas velocity than the actual critical velocity. It would also appear that the correlation is not valid for liquid metals (see Figure 3).

The important characteristics of the various investigations are presented in Table 1 with the symbols which are used in subsequent figures. These data summarized in Table 1 are used to develop the proposed correlations in the subsequent analysis.

In the above discussion several conflicting experimental results, contradictions, and unsolved questions have been pointed out. In order to obtain consistent experimental

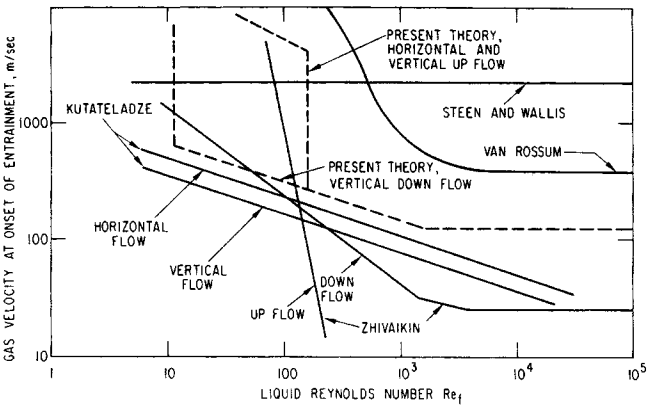


**Fig. 3. Comparison of various correlations for molten stainless steel-sodium vapor at 1430°C and 2.1 atm.**

**Table 1. Summary of Various Experiments on Inception of Entrainment**

| Reference | Fluids* | Geometry | Flow direction | Measurement† | Operational condition | Inception criteria | Symbol used in figure |
|---|---|---|---|---|---|---|---|
| van Rossum (1959) | Water<br>Water +1.5% butanol<br>Water +3.3% butanol<br>Water +7% butanol<br>Kerosene<br>Gas oil<br>Mineral oil 1<br>Mineral oil 2 | Channel 15 × 15 cm | Horizontal | $\delta$, $\Delta P$, $Q_g$, $Q_f$ | Near atmospheric | Visual | |
| Zhivaikin (1962) | Water<br>35% aqueous glycerine<br>47% aqueous glycerine<br>55% aqueous glycerine | 1.3 & 2.1-cm tube | Vertical up and down | $\delta$, $\Delta P$, $Q_g$, $Q_f$ | Near atmospheric | Visual and $\Delta P$ | |
| Wallis (1962) | Water | 10.6 & 1.56-cm tube | Vertical down | Sampling probe $Q_g$, $Q_f$ | Near atmospheric | Linear extrapolation | ○ |
| Steen and Wallis (1964) | Water<br>Ethylene glycol<br>Silicone fluid 96(5)<br>Silicone fluid 96(20) | 1.07 & 10.6-cm<br>1.07-cm tube | Vertical down | Sampling probe $Q_g$, $Q_f$ | 1 atm ~ 4 atm<br>Near atmospheric | Linear extrapolation | ◎⊗◑⊙<br>× |
| Cousin et al. (1965) | Water | 0.953-cm tube | Vertical up | Sampling probe $Q_g$, $Q_f$, $\Delta P$ | 2.72 atm | Zero entrainment | ^ |
| Ueda and Tanaka (1973) | Water | 2.88-cm tube | Vertical down | Sampling probe $Q_g$, $Q_f$, $\Delta P$ | Near atmospheric | Zero entrainment | |
| Yablonik and Khaimov (1972) | Water | 5.8 × 13.6 cm channel with water on wide wall | Vertical down | Sampling probe $Q_g$, $Q_f$ | Near atmospheric | Linear extrapolation | ◇ |
| Present work | Water—nitrogen gas<br>Water—helium gas | 0.318 × 2.54 cm channel with water on wide wall | Inclined down | $\Delta P$, $Q_g$, $Q_f$ | Near atmospheric | $\Delta P$ and visual | ■<br>⊠ |

* Unless otherwise stated, the gas was air.
† $\Delta P$, pressure drop; $Q_g$, volumetric gas flow; $Q_f$, volumetric liquid flow.

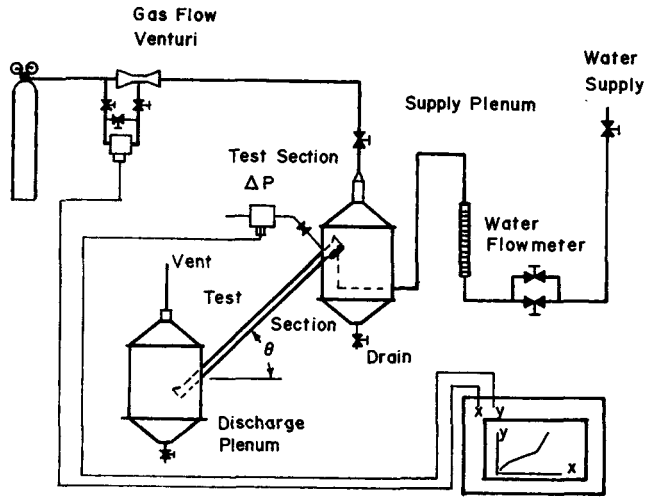


Fig. 4. Gas-liquid entrainment test setup.

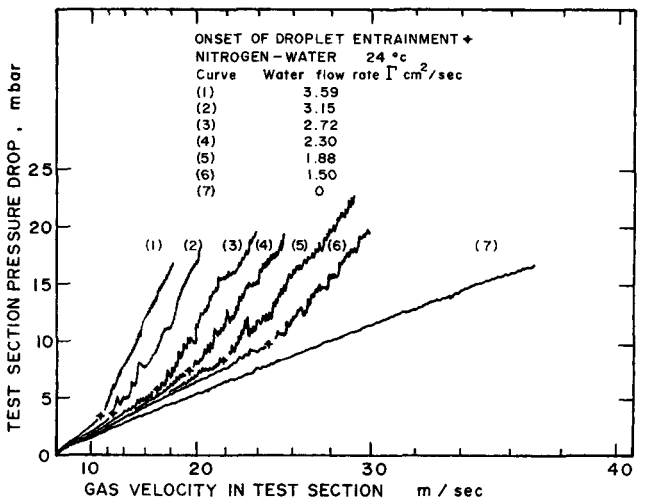


Fig. 5. Test section pressure drop for concurrent gas-liquid flow with onset of droplet entrainment.

data and to eliminate a part of the difficulties associated with the experimental determination of the entrainment inception point, it is necessary to minimize the entrainment caused by the liquid injection to the system. For this purpose, Hewitt and Hall-Taylor (1970) suggests the use of a porous-wall or a suitably designed annular slot as a liquid injector.

The temperature control of a liquid and gas was pointed out to be very important (Zuber, 1962; Amman, 1960), particularly at low temperatures, since for water the liquid viscosity can change considerably. Evidently, additional experimental data with varied gas properties and flow directions under carefully controlled inlet and temperature conditions are needed to resolve some of the existing questions.

## ENTRAINMENT EXPERIMENT

To illustrate some important aspects of the previous discussion, some additional experimental data were obtained in the apparatus shown in Figure 4. A rectangular transparent test section of dimensions 76.2 cm long by 2.54 cm wide by 0.317-cm gap was used. The test section was connected between a supply and receiver plenum and could be elevated at an angle $\theta$ with respect to the horizontal. Data were taken at 45° elevation. Water was smoothly injected through a slot type distributor at the entrance to the test section. The test section ends were tapered 15° to allow for smooth gas flow into and out of the test section. Gas could be directed in either concurrent or countercurrent flow. Both helium and nitrogen were used to permit a 7-fold variation in liquid to vapor density ratio. The onset of droplet entrainment could be observed visually and measured directly as the break in the test section pressure drop vs. gas flow rate curve of Figure 5. Visual and pressure drop measurements were always coincident at the onset of entrainment for initially concurrent flow.

Typical data for concurrent flow are shown in Figure 6. The data illustrate the effect of liquid to vapor density ratio on the onset of entrainment, and for the helium water data, the minimum liquid film thickness or Reynolds number for the cutoff of entrainment. For nitrogen and water, a breakdown in the liquid film to rivulet flow was observed prior to the entrainment cutoff. With the narrow gap height of this test section, entrainment coincided with the flooding transition for initially countercurrent flow because of liquid bridging the total gap at the flooding point. Alternately, for initially concurrent flow, the flooding transition was not observed. Rather, the onset of entrainment was the first flow disruptive transition encountered. These observations point out the various differences between con-and countercurrent flow and the different kinds of behavior at minimum film thickness with regard to breakdown of the flow pattern.

## MECHANISM OF ENTRAINMENT

A wavy liquid film can be entrained into a gas flow in a number of different ways. Hydrodynamic and surface tension forces govern the motion and deformation of the wave crests. Under certain conditions, these forces lead to an extreme deformation of the interface which results in breakup of a portion of a wave into several droplets. The forces acting on the wave crests depend on the flow pattern around them as well as on the shape of the interface. In general, the five basic types of entrainment mechanisms which are shown in Figure 7 can be considered.

In the first type, commonly observed in the experiments (Brodkey, 1967; van Rossum, 1959; Hewitt and Hall-Taylor, 1970; Hanratty and Hershman, 1961), the tops of large amplitude roll waves are sheared off from the wave crests by the turbulent gas flow. The drag force acting on the wave tops deforms the interface against the retaining force of the liquid surface tension.

The second type of entrainment is caused by undercutting the liquid film by a gas flow (Hewitt and Hall-Taylor, 1970). The experimental results of van Rossum (1959) at low Reynolds number are correlated in terms of the Weber number based on the film thickness and show striking simi-

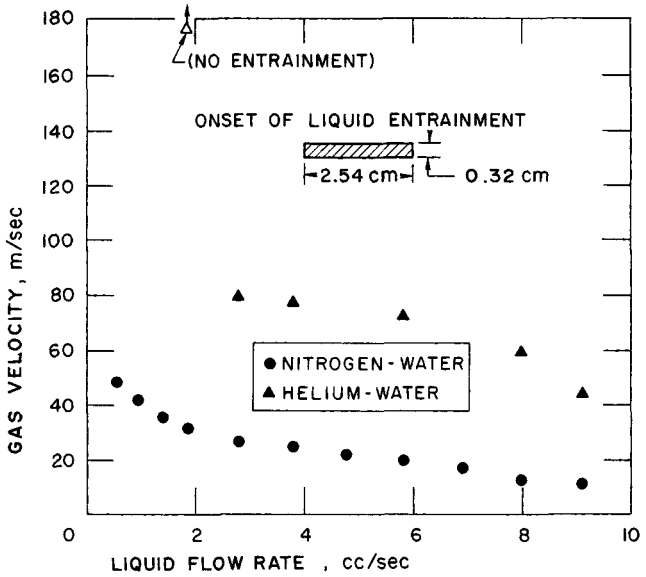


Fig. 6. Data for onset of droplet entrainment.

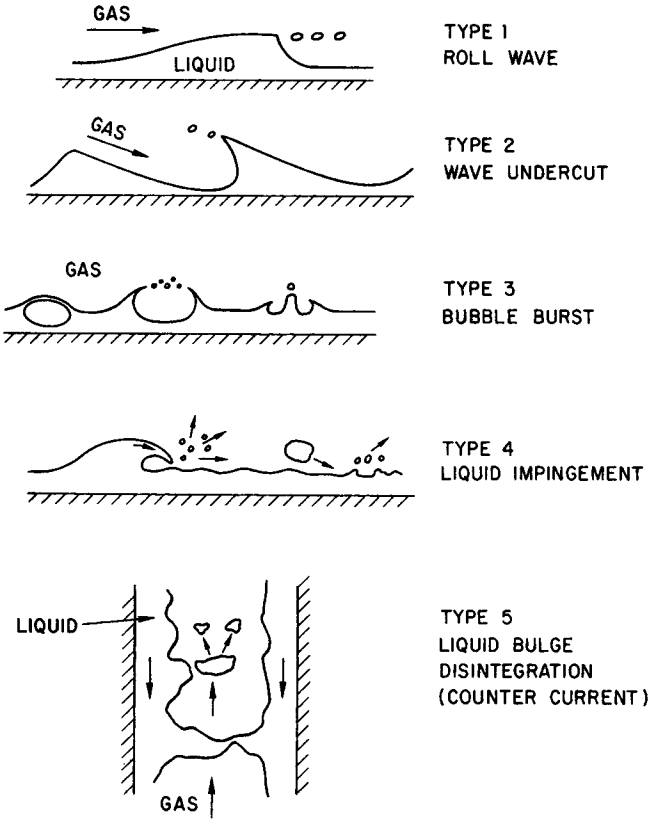


**Fig. 7. Various entrainment mechanisms.**

larity with the criterion of droplet disintegration by a gas stream (Hinze, 1955). Consequently, a strong relation in the breakup mechanism between these two different phenomena can be expected.

The third type is related to the bursting of gas bubbles. It was shown by Newitt et al. (1954) that drops can be generated by a bubble rising to the surface of a liquid. When the bubble reaches the interface, a thin liquid film forms at the top of the bubble which separated it from the gas flow. As the liquid is drained from the film, it eventually ruptures in several places resulting in entrained fine droplets. Much larger drops can be formed on the bursting of bubbles by the motion of the surrounding liquid filling the crater left by the bubble. A spike-like filament rises at the center of the crater which is then disintegrated into droplets. The formation of the bubbles in the liquid film can be due to gas injection, turbulent wavy motions, or nucleation.

The fourth type of entrainment is caused by the impingement of the liquid drops or mass to the film interface. Advancing roll-wave fronts may produce small size droplets by this mechanism.

The last type to be considered here is related to the entrainment associated with the flooding phenomenon. When the countercurrent flow reaches the flooding condition, large amplitude waves can be separated from the film to form a bulge due to the film instability or may even form a liquid bridge between the walls. The formation of the liquid mass in the high velocity gas core flow resembles the experimental condition of droplet disintegration by a gas stream (Hinze, 1955; Sevik and Park, 1973; Sleicher, 1962). It is therefore expected that these liquid buldges and bridges eventually disintegrate into several droplets by the mechanisms discussed by Hinze (1955).

A careful examination of the existing experimental data for the inception of entrainment in concurrent two-phase flow systems, by plotting them on the liquid Reynolds number versus the critical gas velocity plane, indicates that there exist at least three different regimes for each fluid as shown in Figure 8. Here the liquid film Reynolds number is defined by

$$Re_f = \frac{4\rho_f v_f \delta}{\mu_f} = \frac{4\Gamma}{\nu_f} \qquad (1)$$

where $\Gamma$ is the volumetric flow rate per unit wetted perimeter. At large Reynolds numbers, the critical gas velocity becomes practically constant. This gives the minimum gas velocity below which the film entrainment is not possible irrespective of the film Reynolds numbers. The value of $Re_f$ at the boundary between the Reynolds number dependent and Reynolds numbers independent regions lies in the range of 1500 to 2000. This indicates that above this Reynolds number denoted by A in Figure 8, the film is in the completely rough turbulent flow regime in which the hydrodynamics of the film is mostly governed by the interfacial conditions.

In the region between point A and B shown in Figure 8, the critical gas velocity for the onset of entrainment becomes a function of $Re_f$ indicating that the liquid flow within the film also contributes to the momentum exchanges between the phases. Near the inception point of entrainment the interface is very rough; thus it is expected that the quasi-turbulent flow persists to considerably low Reynolds numbers (Hughmark, 1973). The characteristic of this region, therefore, is identified with the laminar-turbulent transition regime.

There are several experimental evidences (van Rossum, 1959; Zhivaikin, 1962; Cousins et al., 1965) showing that below a certain film Reynolds number the critical gas velocity for entrainment starts to increase very rapidly with the decreasing liquid flow rate. Furthermore, the rate of increase of gas velocity is such that for practical purposes it has been identified as an absolute limit of entrainment (Hewitt and Hall-Taylor, 1970). It was assumed there that below this minimum Reynolds number no entrainment is possible irrespective of the gas velocity. Whether the above observed phenomenon really corresponds to the absolute limit or to a rather abrupt transition in the entrainment mechanisms (Zuber, 1962) cannot be resolved completely

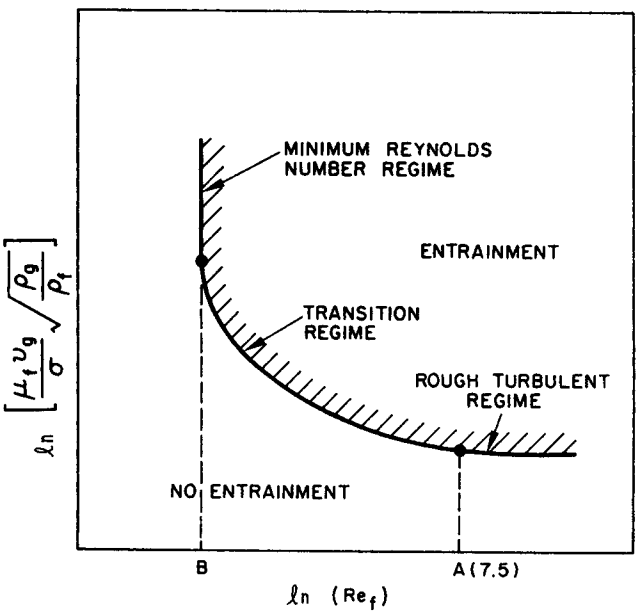


**Fig. 8. Schematic inception boundary for a particular combination of liquid and gas.**

because of the limited experimental data. However, irrespective of the above phenomenon we expect that thinning of the liquid film by the high shear flow of a gas will eventually lead to the submergence of the liquid film in the gas boundary layer. As a consequence, dynamical interaction between the gas turbulence and liquid film is substantially decreased. It can be considered that this leads to the termination of the entrainment. However, the physics of very thin films is further complicated by the appearance of the dry patches due to the poor wettability of the surface (Hartley and Murgatroyd, 1964; Bankoff, 1971). Depending on the surface tension and the contact angle, the continuous film becomes unstable at very small film thickness, and it can break into several rivulets which are the more stable configuration. The hydrodynamics of the small rivulets is expected to be considerably different from that of the continuous film because of the existence of the contact lines.

In the subsequent sections, these three regimes are analyzed separately to obtain the inception criteria for entrainment in concurrent film flows. Since the minimum Reynolds number regime and the rough turbulent regime can be considered as an asymptotic case at each end of the transition regime shown in Figure 8, we first study the entrainment mechanisms in the transition film flow regime.

## TRANSITION REGIME ENTRAINMENT

Of the various entrainment mechanisms discussed in the previous section, the model chosen for the transition film flow regime is shown in Figure 9. It is essentially based on the roll-wave geometry with an internal flow in the wave crest (Type 1 in Figure 7). The amplitude of the wave is denoted by $a$ and the wave length by $\lambda$. Two assumptions concerning the entrainment mechanism and the flow inside the wave crest have been made.

First we assume that the entrainment becomes possible if the drag force $F_d$ from the high shear flow of gas acting on the wave crest exceeds the retaining force of the surface tension $F_\sigma$. Thus, we write

$$F_d \geqq F_\sigma \tag{2}$$

It is noted that this form of the entrainment criterion was

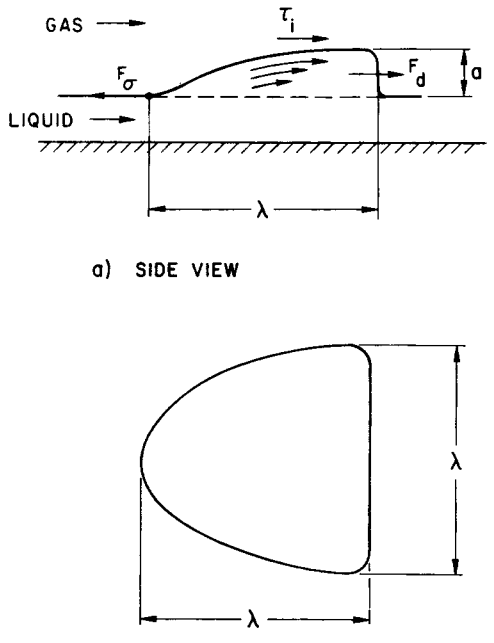


a) SIDE VIEW

b) TOP VIEW

Fig. 9. Model for entrainment based on roll-wave breakup.

first introduced in (Zuber, 1962). Under the above condition, the wave form cannot retain its original form, thus it leads to the deformation of the wave crest. The drag force is given in terms of the drag coefficient $C_d$ as

$$F_d = C_d \lambda a \frac{\rho_g v_r^2}{2} \tag{3}$$

where $v_r$ denotes the relative velocity between the mean gas flow and the film flow. Since the wave crest has a rather deformed shape in comparison with a sphere, the drag coefficient of our interest can be given approximately from the analogy to the drag on an irregular shaped particles. Thus we have

$$C_d \simeq 1 \tag{4}$$

which is applicable to the wave Reynolds number $Re_w = \rho_g v_r a/\mu_g$ in the range of 10 to $5 \times 10^5$ (Brodkey, 1967).

On the other hand, the retaining force of the surface tension is given by

$$F_\sigma = C_s \lambda \sigma \tag{5}$$

where $C_s$ is the interfacial shape coefficient. If the base area of the average wave crest can be approximated by a half ellipse, then we have

$$C_s \lesssim 0.77 \tag{6}$$

Substituting the expressions for the drag force and surface tension into the entrainment criterion (2), we obtain

$$\frac{\rho_g v_r^2 a}{2} \geqq \frac{C_s \sigma}{C_d} \tag{7}$$

The second assumption is concerned with the wave amplitude and the flow within the wave crest. We assume that the interfacial shear force at the top of the wave induces an internal flow of order of magnitude of the film velocity and that the motion of the wave crest with respect to the film can be expressed by a shear flow model:

$$\tau_i = C_w \mu_f \frac{v_f}{a} \tag{8}$$

where $C_w$ is the factor to account for the effect of the surface tension on the internal flow. Since the hydrodynamics inside the wave crest can be described in terms of the viscous force and the surface force, $C_w$ will be a function of these forces. For this reason, we take the following nondimensional form for the expression of $C_w$:

$$C_w = C_w(N_\mu) \tag{9}$$

where the viscosity number $N_\mu$ is given by

$$N_\mu = \frac{\mu_f}{\left(\rho_f \sigma \sqrt{\frac{\sigma}{g\Delta\rho}}\right)^{1/2}} \tag{10}$$

First we note that a similar group has been used by Hinze (1955) to analyze the problem of droplet disintegration in a gas flow. The difference is that an initial droplet diameter was used as a length scale, instead of the one based on the critical wavelength of the Taylor instability used in the present analysis, that is, $\sqrt{\sigma/g\Delta\rho}$, which is also the maximum stable drop radius in the free stream. The physical significance of the group of Hinze was later explained elegantly by Sleicher (1962), by considering the internal flow induced by a natural vibration of the drop. It was shown that the group measures the viscous force induced by an internal flow to the surface tension force. Furthermore, in the field of two-phase analyses, the inverse square of $N_\mu$ is known as the Archimedes number

which has been used to correlate the experimental data in the slug and bubbly flow regimes. The essential point is that the viscosity number is a property group, and thus it does not depend on the flow conditions.

The shear force at the interface can be expressed by either a gas or liquid friction factor as

$$\tau_i = f_{gi}\frac{\rho_g v_r^2}{2} \tag{11}$$

or

$$\tau_i = f_i\frac{\rho_f v_f^2}{2} \tag{12}$$

There are numerous studies on the interfacial friction factors (Levy, 1968; Wallis, 1969; Hewitt and Hall-Taylor, 1970). If the interface is in rough wavy regime, then the simple correlation of Wallis is applicable. Thus,

$$f_{gi} = 0.005\,[1 + 300\,\delta/D] \tag{13}$$

where $D$ is the hydraulic diameter of the duct. On the other hand, a typical expression for the interfacial liquid friction factor $f_i$ can be obtained from the correlation for a film thickness given by Hughmark (1973). Thus, we have

$$\sqrt{f_i} = K\,Re_f^{\,m} \tag{13}$$

where $K$ and $m$ are given by

$$\begin{aligned} &K = 3.73\ , \quad m = -0.47 \text{ for } 2 < Re_f < 100 \\ &K = 1.962, \quad m = -1/3 \text{ for } 100 < Re_f < 1000 \\ &K = 0.735, \quad m = -0.19 \text{ for } 1000 < Re_f \end{aligned} \tag{14}$$

However, the various experimental data used by Hughmark indicate that

$$\sqrt{f_i} = 1.962\,Re_f^{-1/3} \tag{15}$$

is a good estimate for the transition regime explained in the previous section.

Now in view of Equations (8) and (12), the amplitude of the wave can be expressed as

$$a = \sqrt{2}\,C_w(N_\mu)\,\frac{\mu_f}{\rho_f}\sqrt{\frac{\rho_f}{\tau_i}}\,\frac{1}{\sqrt{f_i}} \tag{16}$$

By substituting the above equation into the entrainment criterion given by Equation (7), we get

$$\frac{\mu_f v_r}{\sigma}\sqrt{\frac{\rho_g}{\rho_f}} \geqq 1.96\left[\frac{C_s\sqrt{f_{gi}}}{C_d C_w(N_\mu)}\right] Re_f^{-1/3} \tag{17}$$

Here we have eliminated the liquid friction factor by means of Equation (15). If the previously given expressions for the drag coefficient $C_d$, interfacial shape coefficient $C_s$, and interfacial gas friction factor $f_{gi}$, that is, Equations (4), (6), and (13) are substituted into the above inception criterion, we obtain

$$\frac{\mu_f v_r}{\sigma}\sqrt{\frac{\rho_g}{\rho_f}} = \frac{\sqrt{1 + 300\,\delta/D}}{3\,C_w(N_\mu)}\,Re_f^{-1/3} \tag{18}$$

In addition, if the film thickness is very small such that $\delta/D << 1$, then the relative velocity can be replaced by a gas volumetric flux $j_g$, which is the gas volume flow per unit tube area, and the effect of the film thickness on the friction factor appearing on the right-hand side of the above equation can be neglected. Under the above condition, the simplified form of the inception criterion for entrainment reduces to

$$\frac{\mu_f j_g}{\sigma}\sqrt{\frac{\rho_g}{\rho_f}} \geqq \frac{Re_f^{-1/3}}{3\,C_w(N_\mu)} \tag{19}$$

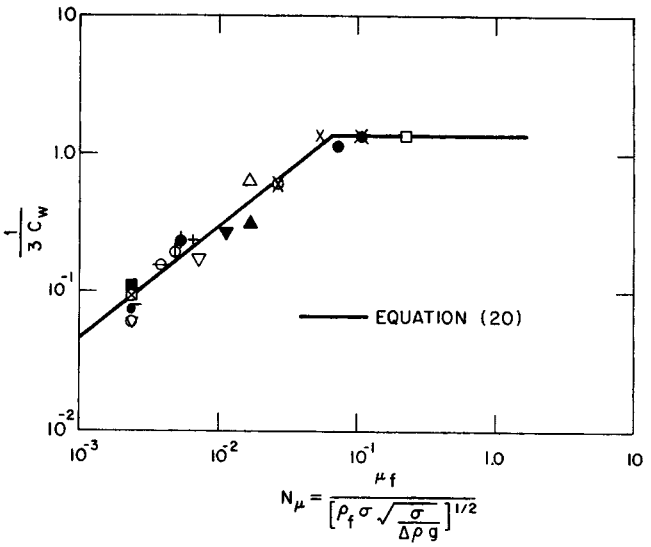


**Fig. 10. Correlation for $C_w$.**

Here the order of magnitude of the coefficient $C_w$ is expected to be one. However, its dependence on the viscosity number $N_\mu$ should be determined from the experimental data because the detailed hydrodynamics inside of the wave crest has not been considered in the present analysis.

The experimental value of $C_w$ for each liquid can be obtained from the full logarithmic plot of the set of data in the plane of the gas velocity group versus the liquid Reynolds number appearing in Equation (19). The position of the straight line with the slope of $-1/3$ best fitted to the data gives the value of $1/(3\,C_w)$. We have used the experimental data listed in Table 1 to determine the functional dependence of $C_w$ on the viscosity number $N_\mu$. The basic characteristics of the data used are shown in Table 1. Figure 10 shows the proposed correlation for $C_w$ and the experimental data used to determine it. Hence, the explicit form of Equation (9) is given by

$$\begin{aligned} \frac{1}{3\,C_w} &= 11.78\,N_\mu^{0.8}; \quad \text{for} \quad N_\mu \leqq \frac{1}{15} \\ &= 1.35 \qquad ; \quad \text{for} \quad N_\mu > \frac{1}{15} \end{aligned} \tag{20}$$

The above relation clearly indicates that in the low viscous number regime surface tension dominates the motion of the liquid within the wave crest whereas for larger viscous number regime, the viscous force controls the motion.

The final form of the simplified inception criterion for entrainment in the transition regime can readily be obtained from Equations (19) and (20), thus we have

$$\begin{cases} \dfrac{\mu_f j_g}{\sigma}\sqrt{\dfrac{\rho_g}{\rho_f}} \geqq 11.78\,N_\mu^{0.8}\,Re_f^{-1/3} & \text{for} \quad N_\mu \leqq \dfrac{1}{15} \\ \geqq 1.35\,Re_f^{-1/3} & \text{for} \quad N_\mu > \dfrac{1}{15} \end{cases} \tag{21}$$

## ROUGH TURBULENT REGIME

For the range where a film Reynolds number exceeds about 1500 to 1750, the film flow becomes completely rough-turbulent and the dependence of the liquid friction factor $f_i$ on $Re_f$ decreases. As a simple approximation, it can be assumed that the liquid friction factor becomes constant for a large Reynolds number in analogy with a flow

over a rough surface. Consequently, in this regime where $Re_f$ exceeds the critical Reynolds number $Re_{fc}$, the inception criterion given by Equation (21) should be rewritten in terms of $Re_{fc}$. By taking the critical Reynolds number to be 1635, the inception criterion for the rough turbulent regime becomes

$$\begin{cases} \dfrac{\mu_f j_g}{\sigma}\sqrt{\dfrac{\rho_g}{\rho_f}} \geqq N_\mu^{0.8}; & \text{for } N_\mu < \dfrac{1}{15}, \quad Re_f > 1635 \\ \geqq 0.1146; & \text{for } N_\mu > \dfrac{1}{15}, \quad Re_f > 1635 \end{cases} \tag{22}$$

The comparison of the above criterion with the experimental asymptotic values of the minimum gas velocity is given in Figure 11. Overall comparisons of the present criteria for the onset of entrainment for weakly viscous fluids, that is, $N_\mu \lesssim 1/15$, to the various experimental data is shown in Figure 12. In view of the previously discussed experimental difficulties in determining the entrainment inception point and the associated scattering of the data, the agreement of the present criteria to the data is satisfactory. The disagreement of the data for the mineral oil no. 3 and gas oil (van Rossum, 1959) with the above criteria is due to the changes in the entrainment mechanisms which will be discussed in the subsequent section.

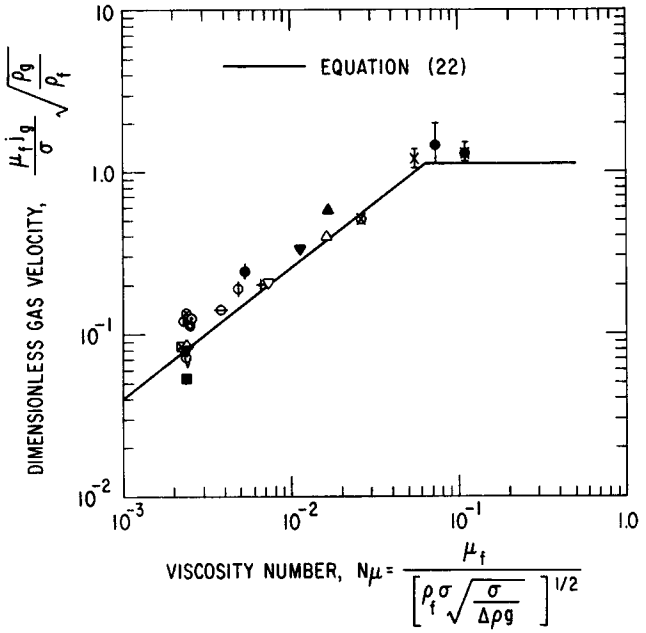


Fig. 11. Comparison of experimental data to predicted minimum gas velocity for inception of entrainment in rough turbulent regime.

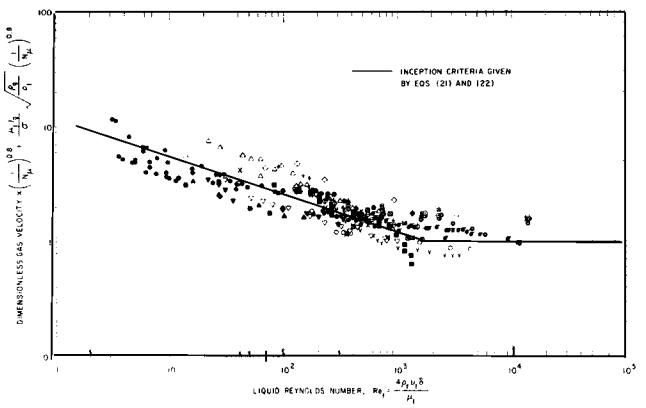


Fig. 12. Comparison of the inception criteria for entrainment based on the roll-wave breakup mechanism to the experimental data.

## LOW REYNOLDS NUMBER ENTRAINMENT

There are considerable theoretical and experimental evidences (Hanratty and Engen, 1957; Hanratty and Hershman, 1961; Brodkey, 1967) indicating that the large amplitude waves having the characteristic of the roll-wave start to disappear for a low Reynolds number film flow. This can be attributed either to the stabilization of the film or to the diminishing growth factor. The value of the Reynolds number corresponding to the roll-wave transition is not firmly established, however, the results of the various investigations suggest that it is in the range of 2 to 5 for a falling liquid film flow. Based on these experimental and theoretical evidence, we assume that the roll-wave entrainment mechanism holds down to the film Reynolds number 2 for a vertical downward liquid flow.

On the other hand, in a horizontal or vertical upward flow, it has been shown that the transition also depends on the gas flow. However, a careful examination of very limited experimental data on the inception of entrainment (van Rossum, 1959; Zhivaikin, 1962; Cousins, 1965) indicates that there exists a sudden deviation from the criterion based on the roll-wave mechanism. The critical gas velocity starts to increase rapidly as the film Reynolds number decreases beyond a certain value. For low viscous fluids, this transition occurs at approximately $Re_f = 160$. This phenomenon can be attributed to the diminishing formation of roll waves due to the decreasing interaction between the gas core turbulent flow and the liquid film. In the absence of sufficient experimental data, we only postulate that the range where the roll-wave entrainment mechanism can be applied is given by

$$\begin{aligned} &Re_f > 2 \quad \text{for vertical down flow} \\ &Re_f > 160 \quad \text{for horizontal or vertical up flow} \end{aligned} \tag{23}$$

Below the above film Reynolds number range, the criterion given by Equation (21) is expected to be increasingly inaccurate. However, this does not exclude the possibility of the entrainment of the liquid into gas stream. Indeed, the experimental data of van Rossum (1959) show that the film entrainment occurs at Reynolds number much less than 160 if the gas velocity is sufficiently high. In this region, it was shown by van Rossum that his data for the inception of entrainment can be well correlated by the film Weber number defined by

$$W_e = \frac{\rho_g v_g^2 \delta}{\sigma} \tag{24}$$

It was shown that the critical Weber number was approximately 17 below which no entrainment existed. This criterion is in startling similarity with the correlations for the droplet disintegration in a gas stream proposed by Hinze (1955) and others (Sevik and Park, 1973; Sleicher, 1962). Using the droplet Weber number based on the initial diameter of a drop instead of the film thickness $\delta$ used in Equation (24), Hinze discussed three different disintegration mechanisms. For a relatively low viscosity fluid, the critical Weber number is found to be 12 if the drop is exposed to a sudden gas flow, whereas for a falling drop, it is approximately 22. The critical Weber number increases with increasing viscosity. On the other hand, in a highly turbulent flow, a drop can disintegrate at much smaller Weber number due to turbulent energy transfer. During the breakup process, it has been observed that the drop undergoes stages of extreme flattening, formation of

a half cup shaped air bag, increasing bag size, and thinning of the film, bursting of the film to produce very fine droplets, and breakup of the base into larger drops.

In the case of a film entrainment at low Reynolds numbers, it is possible that a similar process is initiated by a gas turbulence which acts on the film to undercut it as discussed in the previous section. The photographic study of van Rossum (1959) apparently supports this entrainment mechanism. If the complete similarity exists between the droplet disintegration and the film entrainment, then we have

$$\frac{\rho_g \delta v_r^2}{\sigma} \geq C \tag{25}$$

Here we consider that the value of $C$ should include the effect of the solid wall on the length scale represented by the film thickness. The proposed correlation of van Rossum (1959) gives this constant to be 17 which is reasonably close to the value 22 obtained by Hinze (1955).

As noted by van Rossum, the above criterion is difficult to apply to practical cases because usually the film thickness is not known. For this reason, he gave a film thickness correlation based on the laminar flow model. The essential point of the correlation is that the mean film thickness is 0.6 times the one based on the smooth laminar film and the dry wall shear stress. Because the correlation of van Rossum is somehow cumbersome to use, we propose here an alternative correlation.

The film correlation of Hewitt and Hall-Taylor (1970) and Hughmark (1973) show that if the interfacial shear stress is used instead of dry wall shear stress, then the liquid friction factor is almost the same function of the liquid Reynolds number as it is for a single-phase laminar flow. By using this result, the film thickness can be given by

$$\left(\frac{\delta \rho_f}{\mu_f}\right)\sqrt{\frac{\tau_{gi}}{\rho_f}} = \frac{1}{\sqrt{2}} Re_f^{1/2} \tag{26}$$

The shear stress in the above expression can be replaced by the interfacial gas friction factor $f_{gi}$, thus the inception criterion of entrainment, Equation (25), can be rewritten as

$$\frac{\mu_f v_r}{\sigma}\sqrt{\frac{\rho_g}{\rho_f}} \geq C\sqrt{f_{gi}}\, Re_f^{-1/2} \tag{27}$$

If the value of $C$ is taken as the one given by Hinze for the droplet disintegration, that is, $C = 22$, and the film thickness is assumed to be very small as in the previous case, the criterion reduces to

$$\frac{\mu_f j_g}{\sigma}\sqrt{\frac{\rho_g}{\rho_f}} \geq 1.5\, Re_f^{-1/2} \tag{28}$$

The above correlation is applicable to the range of $Re_f < 2$ for a vertical downwards flow and $Re_f < 160$ for a horizontal or vertical upwards flow.

The comparison of the above inception criterion for entrainment is compared to the available experimental data in Figure 13.

It can be seen from the figure that the criterion based on the wave-undercut mechanism agrees with the experimental data better than the one based on the roll-wave mechanism in the applicable Reynolds number range. Furthermore, the clear transition in the entrainment mechanisms can be seen at $Re_f$ approximately 160 for the vertical upward and horizontal flow.

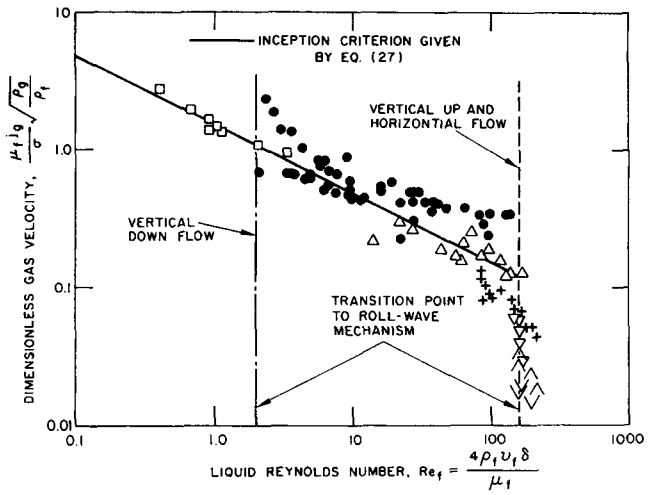


**Fig. 13. Comparison of the inception criterion for entrainment based on the wave-undercut mechanism to the experimental data.**

## MINIMUM REYNOLDS NUMBER

In order to have a full dynamic interaction between the turbulent gas core and the film, the wave should penetrate through the gas boundary layer. By taking into consideration that the order of magnitude of the maximum amplitude is about two to four times of the film thickness for a relatively thin film (Hewitt and Hall-Taylor, 1970; Wallis, 1969; Chung and Murgatroyd, 1965; Gill and Hewitt, 1966), the energy transfer from the gas turbulence to the liquid can be characterized by the ratio of the film thickness $\delta$ and the gas boundary layer thickness. The length scale associated with the boundary layer can be given by

$$l = y^+ \frac{\mu_g}{\rho_g}\sqrt{\frac{\rho_g}{\tau_i}} \tag{29}$$

where $y^+$ represents the dimensionless distance from the wall based on the shear velocity. For example, if $y^+ = 5$ then $l$ gives the thickness of the laminar sublayer. An appropriate expression for the film thickness can be obtained from Equation (1), (12), and (15) by eliminating $v_f$ and $f_i$, thus

$$\delta = 0.347\, Re_f^{2/3}\sqrt{\frac{\rho_f}{\tau_i}}\frac{\mu_f}{\rho_f} \tag{30}$$

The minimum Reynolds number criterion can be obtained by postulating that for $\delta < l$ no entrainment can be possible. In other words from Equations (29) and (30), we have

$$(Re_f)_{\min} = \left(\frac{y^+}{0.347}\right)^{3/2}\left(\frac{\rho_f}{\rho_g}\right)^{3/4}\left(\frac{\mu_g}{\mu_f}\right)^{3/2} \tag{31}$$

The above minimum Reynolds number sets the absolute limit on the onset of entrainment below which no entrainment is possible irrespective of the gas velocity. In view of very limited experimental data, the value of $y^+$ cannot be established firmly; however, the amplitude-film thickness relation and the standard boundary layer theory indicate that $y^+$ is in the range of 30/2 to 30/4 where 30 stands for the thickness of the sublayer and the buffer layer. By taking the mean value, we have

$$y^+ \doteq 10 \tag{32}$$

## SUMMARY OF THE CRITERIA

Summarizing the results obtained above, it can be said that in general one has to know the liquid flow direction, liquid Reynolds number $Re_f$, and the viscosity number $N_\mu$

in order to predict the critical gas velocity. In the rough turbulent regime, $Re_f > 1635$, the onset of entrainment criterion is given by Equation (22) which is the asymptotic case of the one based on the roll-wave mechanism, and it can be applied irrespective of the liquid flow direction.

The entrainment inception criterion, Equation (21), has been obtained by considering the shearing off of roll-wave crests, and it is applicable in the range $160 < Re_f < 1635$ for the horizontal or vertical upwards flow and $2 < Re_f < 1635$ for the downward flow. At the lower limits of the Reynolds number, the entrainment mechanism shifts abruptly to the one based on the wave undercutting mechanism, Equation (28). In addition to the inception of entrainment criteria, the minimum Reynolds number criterion, Equation (31), sets the absolute limit on the onset of entrainment.


## ACKNOWLEDGMENTS

The authors would like to express their appreciation to Dr N. Zuber of AEC for the valuable discussions on the subject, to G. A. Lambert for the performance of the experiment, and to Debbie Lambert for her excellent typing of the manuscript. The constructive criticism on the manuscript by T. C. Chawla is also appreciated.

This work was performed under the auspices of the U. S. Atomic Energy Commission.


## NOTATION

$a$ = roll wave amplitude, cm
$C$ = coefficient for Weber number criterion
$C_d$ = drag coefficient
$C_s$ = interfacial shape coefficient
$C_w$ = coefficient for internal flow
$D$ = hydraulic diameter
$f_{gi}$ = gas interfacial friction factor
$f_i$ = liquid interfacial friction factor
$F_d$ = drag force, dyne
$F_\sigma$ = surface tension force, dyne
$g$ = acceleration of gravity
$j_g$ = gas volumetric flux, that is, superficial gas velocity, cm/s
$K$ = factor in Hughmark interface friction factor correlation
$l$ = boundary layer length scale, cm
$m$ = a constant given by Equation (14)
$N_\mu$ = viscosity number defined by Equation (10)
$Re_f$ = film Reynolds number defined by Equation (1)
$Re_w$ = wave Reynolds number, $\rho_g v_r a/\mu_g$
$v_f$ = liquid film velocity, cm/s
$v_g$ = gas velocity, cm/s
$v_r$ = relative velocity between phases, cm/s
$We$ = Weber number
$y^+$ = nondimensional distance from wall

### Greek Letters

$\Gamma$ = liquid volume flow rate per unit of wetted perimeter, $cm^2/s$
$\Delta\rho$ = density difference, $g/cm^3$
$\delta$ = average film thickness, cm
$\lambda$ = roll-wave length, cm
$\nu_f$ = kinematic viscosity of liquid, cm/s
$\mu_f$ = liquid viscosity, g/cm s
$\mu_g$ = gas viscosity, g/cm s
$\rho_f$ = liquid density, $g/cm^3$
$\rho_g$ = gas density, $g/cm^3$
$\sigma$ = surface tension, dyne/cm
$\tau_i$ = interfacial shear stress, $dyne/cm^2$

## LITERATURE CITED


Amman, H. R., "Viscosity Effects in Two-Phase Annular Flow," M.Sc. thesis, Purdue Univ., West Ind. (1960).

Bankoff, S. G., "Minimum Thickness of a Draining Liquid Film," *Intern. J. Heat Mass Transfer*, **14**, 2143 (1971).

Brodkey, R. S., *The Phenomena of Fluid Motions*, pp. 112-115, 489, 561-565, Addison-Wesley, Reading, Mass. (1967).

Chien, S. F., and W. Ibele, "Pressure Drop and Liquid Film Thickness of Two-Phase Annular and Annular-Mist Flows," ASME Paper 62-WA-170 (1960).

Chung, H. S., and W. Murgatroyd, "Studies of the Mechanism of Roll Wave Formation on Thin Liquid Films," paper presented at Symp. on Two-Phase Flow, Exter, England (1965).

Collier, J. G., "Burnout in Liquid Cooled Reactors," *Nuclear Power*, V, 61 (May 1961).

Cousins, L. B., W. H. Denton, and G. F. Hewitt, "Liquid Mass Transfer in Annular Two-phase Flow," paper presented at Symp. on Two-Phase Flow, Exter, England (1965).

Duffey, R., "The Physics of Rewetting in Water Reactor Emergency Core Cooling," *Nuc. Eng. Design*, **25**, 379 (1973).

Gill, L. E., and G. F. Hewitt, "Sampling Probe Studies of the Gas Core in Annular Two-Phase Flow III," UKAEA Report AERE-M 1202 (1966).

Grolmes, M. A., G. A. Lambert, and H. K. Fauske, "Flooding Correlation for Sodium and Cladding Motion in Subassembly Voiding," *Trans. Am. Nuclear Soc.*, **18**, 209 (1974).

Hanratty, T. J. and J. M. Engen, "Interaction Between a Turbulent Air Stream and a Moving Water Surface," *AIChE J.*, **3**, 299 (1957).

Hanratty, T. J., and A. Hershman, "Initiation of Roll Waves," *ibid.*, **7**, 488 (1961).

Hartley, D. E., and W. Murgatroyd, "Criteria for the Breakup of Thin Liquid Layers Flowing Isothermally Over Solid Surfaces," *Intern. J. Heat Mass Transfer*, **7**, 1003 (1964).

Henry, R. E., W. C. Jeans, D. J. Quinn, and E. A. Spleha, "Cladding Relocation Experiments," *Trans. Am. Nuclear Soc.*, **18**, 209 (1974).

Hewitt, G. F., and N. S. Hall-Taylor, *Annular Two-Phase Flow*, pp. 136-148, Pergamon Press, N. Y. (1970).

Hinze, J. O., "Fundamentals of the Hydrodynamic Mechanism of Splitting in Dispersion Process," *AIChE J.*, **1**, 289 (1955).

Hughmark, G. A., "Film Thickness, Entrainment, and Pressure Drop in Upward Annular and Dispersed Flow," *AIChE J.*, **19**, 1062 (1973).

Kinney, G. R., A. E. Abramson, and J. S. Sloop, "Internal-Liquid Film Cooling Experiments with Air Stream Temperature to 2000°F in 2 and 4 Inch Diameter Horizontal Tubes," NACA Rept. 1087 (1957).

Knuth, E. L., "The Mechanics of Film Cooling Part I and II," *Jet Propulsion*, 359 (1954) 16 (1955).

Kutaleladze, S. S., "Elements of the Hydrodynamics of Gas-Liquid System," *Fluid Mech.-Soviet Res.*, **1**(4), 29 (1972).

Lamb, H., "Hydrodynamics," p. 456-464, p. 363-475 Dover, N. Y. (1945).

Levich, V. G., "Physicochemical Hydrodynamics," pp. 591-626, 683-692, 395-404, Prentice-Hall, N. Y. (1962).

Levy, S., "Prediction of Two-Phase Annular Flow with Liquid Entrainment," *Intern. J. Heat Mass Transfer*, **9**, 171 (1966).

Lighthill, M. J., and G. B. Whitham, "On Kinematic Waves I and II," *Proc. Royal Soc. London, Ser. A*, **229**, 281 (1955).

Newitt, D. M., N. Dombrowski, and F. H. Knelman, "Liquid Entraninment: I, The Mechanism of Drop Formation from Gas or Vapor Bubbles," *Trans. Inst. Chem. Eng.*, **32**, 244 (1954).

Petrovichev, V. I., L. S. Kokorev, A. Ya. Didenko, and G. P. Dubvrovskiy, "Droplet Entrainment in Boiling of Thin Liquid Film," *Heat Transfer—Soviet Res.*, **3**(1), 19 (1971).

Pushkina, O. L., and Yu. L. Sorokin, "Breakdown of Liquid Film Motion in Vertical Tubes," *ibid.*, **1**(5), 56 (1969).

Semeria, R., and B. Martinet, "Calefaction Spots on a Heating Wall; Temperature Distribution and Resorption," paper presented at Symp. on Boiling Heat Transfer in Steam Generating Unit and Heat Exchangers, Manchester (1965).

Sevik, M., and S. Park, "The Splitting of Drops and Bubbles by Turbulent Fluid Flow," *J. Fluid Eng.*, **53** (1973).

Sleicher, Jr., C. A., "Maximum Stable Droplet Size in Turbulent Flow," *AIChE J.*, 8, 471 (1972).
Steen, D. A., and G. B. Wallis, "The Transition from Annular to Annular-Mist Cocurrent Two-Phase Down Flow," AEC Report NYO-3114-2 (1964).
Ueda, T., and T. Tanaka, "Studies of Liquid Film Flow in Two-Phase Annular and Annular-Mist Flow Regions, Part 1 and 2," *Trans. JSME*, **39**, No. 325, 2842 (1973).
van Rossum, J. J., "Experimental Investigation of Horizontal Liquid Films," *Chem. Eng. Sci.*, **11**, 35 (1959).
Wallis, G. B., "The Onset of Droplet Entrainment in Annular Gas-Liquid Flow," General Electric Report 62 GL 127 (1962).
———., *One-Dimensional Two-Phase Flow*, pp. 320, 345-351, 376-391, McGraw-Hill, N. Y. (1969).
Yablonik, R. M., and V. A. Khaimov, "Determination of the Velocity of Inception of Droplet Entrainment in Two-Phase Flow," Fluid Mech. *Societ Res.* **1**(1), 130 (1972).
Yamanouchi, A., "Effects of Core Spray Cooling at Stationary State After Loss of Coolant Accident," *J. Nuclear Sci. Tech.*, 5(9), 498 (1968).
Zhivaikin, L. Ya., "Liquid Film Thickness in Film-Type Units," *Intern. Chem. Eng.*, **2**(3), 337 (1962).
Zuber, N., "On the Atomization and Entrainment of Liquid Films in Shear Flow," General Electric Co. Report 62 GL 153 (1962).

*Manuscript received September 26, 1974; revision received November 25 and accepted November 29, 1974.*

# Steady State Multiplicity of Adiabatic Gas-Liquid Reactors:

## I. The Single Reaction Case

A model of an adiabatic continuously stirred-tank reactor in which a single exothermic second order-gas liquid reaction occurs has been developed. The interactions between the rate of the chemical reaction, the diffusional resistances, and the solubility may cause the occurrence of up to five steady state solutions, even though no more than three solutions can be attained when the same reaction is carried out in a single phase CSTR. A parametric study is used to examine the sensitivity of the model to the value of several parameters. Topological arguments are used to obtain a simple instability criterion.

**LEE A. HOFFMAN**
**SHANMUK SHARMA**
**and DAN LUSS**

**Department of Chemical Engineering**
**University of Houston**
**Houston, Texas 77004**

## SCOPE

Many important gas-liquid reactions such as chlorination, oxidation, and hydrogenation are carried out in a CSTR (continuously stirred-tank reactor). The interactions among the various physical and chemical rate processes in these reactors may cause the occurrence of steady state multiplicity as observed by Ding et al. (1974) and of unusual dynamic phenomena such as sustained periodic oscillation (Hancock and Kenney, 1972).

Theoretical analyses of the steady state multiplicity and stability of a two-phase CSTR have been presented by Schmitz and Amundson (1963a,b,c,d) and Luss and Amundson (1967) using mathematical models which assume that the chemical reaction and the interphase mass transfer are two independent noninteracting processes. However, this description does not properly account for the actual rate of reaction (or absorption) of gaseous reactant species except when the mass transfer resistance is negligible. For example, this formulation fails to account for the enhancement of the mass transfer coefficient by the chemical reaction when the mass transfer rate is the controlling resistance. Recent experiments carried out in our laboratory indicate that these simplified models are often capable of predicting many of the qualitative features of gas-liquid reactors. However, they are inadequate for a quantitative simulation of the behavior of a CSTR over a wide range of temperatures in which a continuous shift from chemical to mass transfer control occurs.